Article

The Thermodynamics of the Transformation of Graphite to Multiwalled Carbon Nanotubes

Daniele Gozzi, Massimiliano Iervolino, and Alessandro Latini

J. Am. Chem. Soc., **2007**, 129 (33), 10269-10275• DOI: 10.1021/ja072120d • Publication Date (Web): 01 August 2007

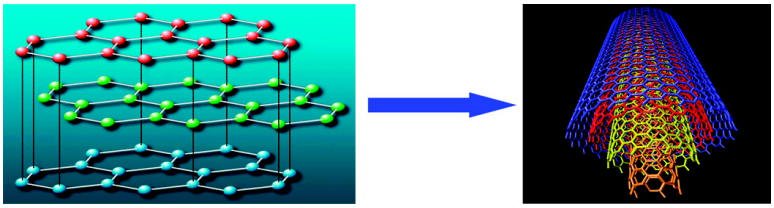

J|A|C|S
ARTICLES
Published on Web 08/01/2007

The Thermodynamics of the Transformation of Graphite to Multiwalled Carbon Nanotubes

Daniele Gozzi,* Massimiliano Iervolino, and Alessandro Latini

Contribution from the Dipartimento di Chimica, Università di Roma "La Sapienza", Piazzale Aldo Moro 5, 00185 Roma, Italy

Received March 26, 2007; E-mail: daniele.gozzi@uniroma1.it

Abstract: The thermodynamic quantities associated to the transformation from graphite to multiwalled carbon nanotubes (MWCNTs) were determined by electromotive force (emf) and differential scanning calorimetry (DSC) measurements. From the emf versus T data of galvanic cell Mo|Cr_3C_2, CrF_2, MWCNTs|CaF_2 s.c.|Cr_3C_2, CrF_2, graphite|Mo with CaF_2 as solid electrolyte, $\Delta_r H^o_{\bar{T}} = 8.25 \pm 0.09$ kJ mol^{-1} and $\Delta_r S^o_{\bar{T}} = 11.72 \pm 0.09$ JK^{-1} mol^{-1} were found at average temperature $\bar{T} = 874$ K. The transformation enthalpy was also measured by DSC of the Mn_7C_3 formation starting from graphite or MWCNTs. Thermodynamic values at 298 K were calculated to be: $\Delta_r H^o_{298} = 9.0 \pm 0.8$ kJ mol^{-1} as averaged value from both techniques and $\Delta_r S^o_{298} \approx \Delta_r S^o_{\bar{T}}$. At absolute zero, the residual entropy of MWCNTs was estimated 11.63 ± 0.09 JK^{-1} mol^{-1}, and transformation enthalpy $\Delta_r H^o_0 \approx \Delta_r H^o_{298}$. The latter agrees satisfactorily with the theoretical calculations for the graphite−MWCNTs transformation. On thermodynamic basis, the transformation becomes spontaneous above 704 ± 13 K.

1. Introduction

Since the discovery of the carbon nanotubes (CNTs) in 1991 by Iijima,[1] the scientific community showed an even more growing interest in this allotropic form of carbon and many papers covering basic[2,3] and theoretical[4,5] aspects as well as applications[6,7] were published. It is usual to distinguish CNTs in single-walled (SWCNTs) and multiwalled (MWCNTs) depending on how many graphene planes are coaxially assembled.

Graphite represents the reference state of any type of CNTs, graphite being the stable form of carbon resulting from the assembling of graphene planes piled up along the orthogonal *c*-axis. A weak interlayer energy, W_L, ranging from 4.10^8 to 21.0^9 kJ mol^{-1}, holds together the graphene plane, whereas a strong C−C bond energy, W_B, links carbon atoms in the planes. Any deviation from the planarity increases the energy of the assembly of the graphene layers, which depends on the distance between layers and the bending of the sp^2 planar bond structure. CNTs result from so large a deviation from the planarity of the assembly of graphene planes such as to form a cylindrical shape. Therefore, it is expected that the energy content of the CNTs is higher than graphite.

Some theoretical approaches[10,11] are reported in literature to calculate the CNT energy as function of the size of the diameter and length and as function of the number of walls in the case of MWCNTs. As far as to the authors' knowledge, no experimental measurement has been reported to determine the thermodynamic quantities, such as the changes of the standard free energy, $\Delta_r G^o$, the standard enthalpy, $\Delta_r H^o$, and the standard entropy, $\Delta_r S^o$, related to the transformation from graphite to MWCNTs. This can be explained by the difficulty in obtaining MWCNTs in a reasonable quantity without amorphous and/or graphitic carbon as well as by the intrinsic difficulty in determining the thermodynamic properties. The purity is not the unique necessary requirement to be searched for MWCNTs. The quantities length, diameter, number of walls, and defectivity should be known too. All this information is generally unknown or when some of it is available, it is not representative of the whole mass of sample under study. The availability of sufficient amorphous carbon-free amounts of MWCNTs, grown from methane decomposition on a patent catalyst,[12] allowed a reliable and repetitive experimentation. The absence of amorphous carbon and a satisfactory uniformity in sizes and number of walls are explained by the peculiar nucleation and growth mechanism[13] due to the catalyst and low temperature (∼500 °C) at which MWCNTs grow.

For several years, the electromotive force (emf) technique using solid-state galvanic cells is routinely practiced in our laboratory, and more recently the technique has been utilized particularly for determining the thermodynamic properties of

(1) Iijima, S. *Nature* **1991**, *354*, 56.
(2) Belin, T.; Epron, F. *Mater. Sci. Eng. B* **2005**, *119*, 105.
(3) Harris, J. F. *Carbon* **2007**, *45*, 229.
(4) Sun, C. H.; Finnerty, J. J.; Lu, G. Q.; Cheng, H. M. *J. Phys. Chem. B* **2005**, *109*, 12406.
(5) Reich, S.; Li, L.; Robertson, J. *Phys. Rev. B* **2005**, *72*, 165423.
(6) Tasis, D.; Tagmatarchis, N.; Bianco, A.; Prato, M. *Chem. Rev.* **2006**, *106*, 1105.
(7) Raffaelle, R. P.; Laudi, B. J.; Harris, J. D.; Bailey, S. G.; Hepp, A. F. *Mater. Sci. Eng. B* **2005**, *116*, 233.
(8) Girifalco, L. A. Ph.D. Thesis. University of Cincinnati, Clincinnati, OH, 1954.
(9) Setton, R. *Bull. Soc. Chim. Fr.* **1960**, *1758*, 521.
(10) Setton, R. *Carbon* **1996**, *34*, 69.
(11) Zhang, S.; Zhao, S.; Xia, M.; Zhang, E.; Xu, T. *Phys. Rev. B* **2003**, *68*, 245419.
(12) Gozzi, D.; Latini, A. Patent No. 05802229.4-2111-IT2005000587.
(13) Tomellini, M.; Gozzi, D.; Latini, A. *J. Phys. Chem. C* **2007**, *111*, 3266.

10.1021/ja072120d CCC: $37.00

binary intermetallics with rare-earth and transition metals.[14,15] The thermodynamic properties of the graphite−MWCNTs transformation were determined through the electromotive force measurements versus temperature of galvanic cells with CaF_2 single crystal as solid electrolyte. In the present case, to support by an independent technique the reliability of the data obtained through emf measurements (reversible technique), $\Delta_r H^o$ has been measured also by differential scanning calorimetry, DSC (irreversible technique).

2. Experimental

2.1. Synthesis of MWCNTs and Characterization. MWCNTs were grown by catalytic decomposition of methane over a patent pending catalyst.[12] They were purified by removing the catalyst by two acid treatments always under magnetic stirring, initially with hot concentrated HCl and, after filtering on a gooch funnel, with a 1:1 mixture of hot water and concentrated HCl. The suspension was again filtered on a gooch funnel, washed with deionized water up to pH ≈ 7 and then washed with acetone. The solid was left some minutes under suction to dry, then was placed in an oven and held at 150 °C to remove the adsorbed water. Extended observations by SEM and TEM do not show forms of carbon other than CNTs. Typical SEM and TEM images of MWCNTs are reported in Figure 1a−c. The distribution of outer and inner diameter and number of MWCNT walls was found almost uniform as expected from their growth mechanism.[13] The average values of the inner and outer diameters and the length were found to be 4 nm, 130 nm, and 10 μm, respectively. Therefore, the number of walls has to be considered very high being that the spacing between the walls is practically equal to the spacing between the graphene planes of graphite. This is generally recognized for MWCNTs of large outer diameter.

The carbon content, evaluated by thermogravimetric (TG) analysis (Netzsch STA 409 PC Luxx, resolution 2 μg) in pure oxygen (Figure 2), is greater than 98.68 wt % as found by the TG weight loss. Since some traces of catalyst, which gain weight during the oxidation, are present in the MWCNTs, the true carbon content is 98.94 wt %.

Raman spectroscopy was also utilized to characterize the synthesized MWCNTs. Figure 3 shows the fingerprint bands of MWCNTs in the first- and second-order spectra. According to the literature,[16] because of defectivity, MWCNTs display in the first-order spectrum a higher intensity of the D band with respect to graphite, whereas the G bands remain practically unchanged. The second-order spectrum is characterized by a more intense G'_1 and D + G bands with respect to graphite.

2.2. Galvanic Cells. The electrochemical cell with CaF_2 single crystal (s.c.) as solid electrolyte has been adopted:

$$\text{low} - \text{Mo}/\text{Cr}_3\text{C}_2,\text{CrF}_2,\text{C}''/\text{CaF}_2\text{s.c.}/\text{Cr}_3\text{C}_2,\text{CrF}_2,\text{C}'/\text{Mo} - \text{high} \quad \text{(A)}$$

where C′ and C″ are two allotropic forms of carbon.

The electrode containing carbon as graphite was already studied[17] in galvanic cells for determining the thermodynamic properties of Cr_3C_2 in combination with reference electrode Cr−CrF_2. Cell A is a fluorine concentration cell where the positive electrode is the electrode where the chemical potential of F_2(g) is higher. The cell reaction can be written as

$$3e + \frac{3}{2}\,\text{CrF}_2 + \text{C}' = 3\text{F}^- + \frac{1}{2}\,\text{Cr}_3\text{C}_2\text{:}(+)$$

$$3\text{F}^- + \frac{1}{2}\,\text{Cr}_3\text{C}_2 = 3e + \frac{3}{2}\,\text{CrF}_2 + \text{C}''\text{:}(-)$$

$$\text{C}' = \text{C}'' \qquad \text{(B)}$$

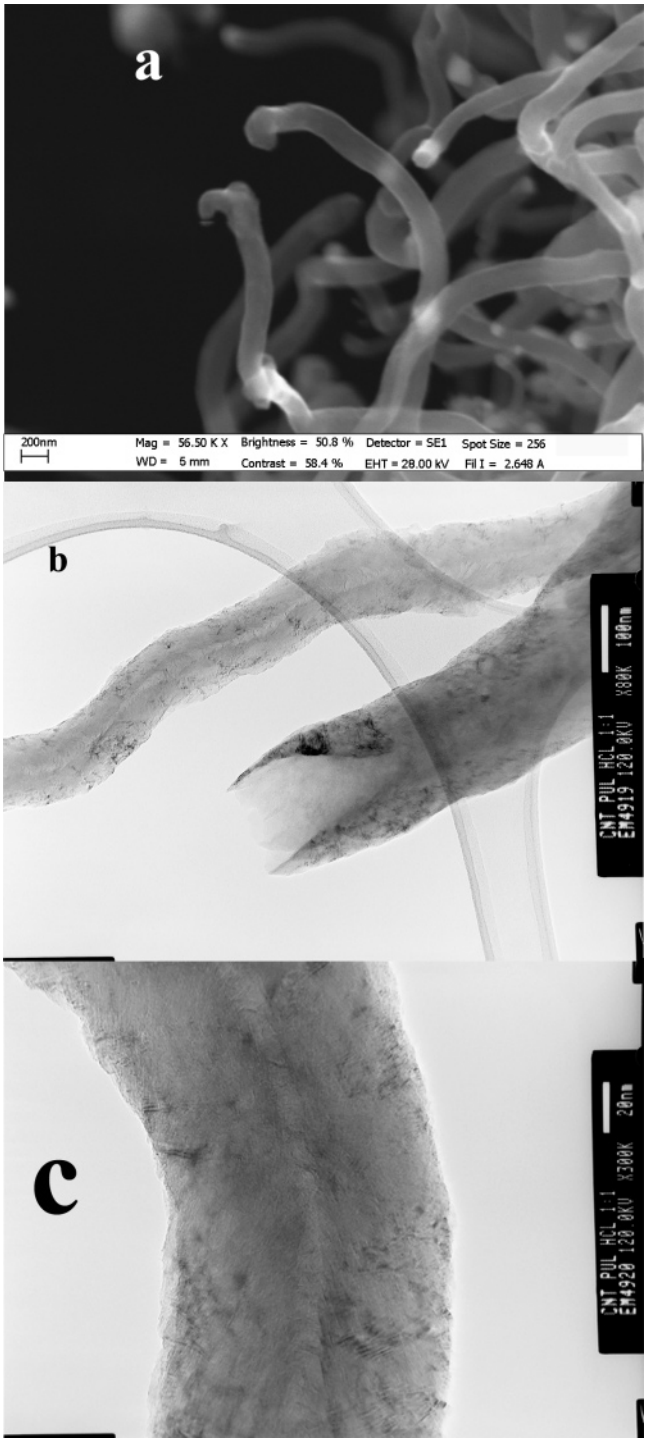

Figure 1. (a) Scanning electron microscopy (SEM) photo of MWCNTs. (b) Transmission electron microscopy (TEM) photo of a few MWCNTs purified by the catalyst nanoparticles. One of the ends of a nanotube is shown. The pristine shape of the catalyst nanoparticle is maintained. (c) TEM photo showing the innermost tube diameter ≈ 4 nm.

The main advantage of this kind of cells is that no supplementary thermodynamic data are necessary to derive the thermodynamics of the cell reaction. Only the emf versus T experimental data are necessary to obtain $\Delta_r G^o$, $\Delta_r H^o$, and $\Delta_r S^o$ as reported in any chemical thermodynamics textbook.

(14) Di Pascasio, F.; Gozzi, D.; Parodi, N.; Borzone, G. *J. Phys. Chem. B* **2002**, *106*, 4284.
(15) Gozzi, D.; Iervolino, M. *Intermetallics* **2005**, *13*, 1172.
(16) Antunes, E. F.; Lobo, A. O.; Corat, E. J.; Trava-Airoldi, V. J.; Martin, A. A.; Verissimo, C. *Carbon* **2006**, *44*, 2202.
(17) Kleykamp, H. *J. Alloy Compd.* **2001**, *321*, 138.

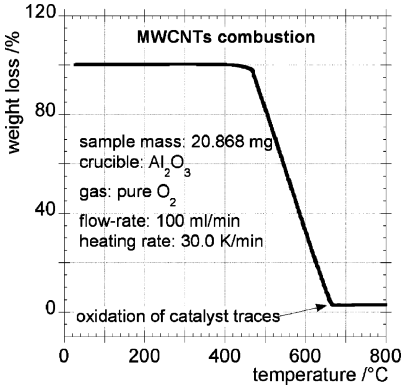

Figure 2. Combustion analysis of MWCNTs by thermogravimetry (TG). The carbon content is 98.94 wt %. The impurity is constituted by catalyst traces.

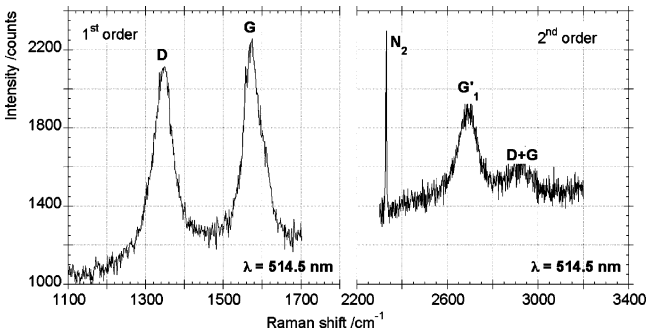

Figure 3. First- and second-order Raman spectra of the synthesized MWCNTs at the 514.5 nm excitation source wavelength.

2.2.1. Cell Assembly. All the details of the experimental setup are reported in literature.[14,15] Only essential information will be reported here.

The emf measurements were carried out in a high-vacuum vertical furnace using an inconel spring-loaded latticework for positioning the holder of the electrochemical cell in the isothermal zone of the furnace. The vertical force applied to the cell is maintained at a preset value by a feedback motion to compensate the size changes due to the temperature variations. In this way the contact pressure at the electrode/electrolyte interface is independent of the temperature. The cell holder containing the electrodes, electrolyte, and Mo lead wires is machined from a workable alumina rod (Aremco). Two small holes (1 mm diameter) serve as an outlet for the Mo wires and cell out-gassing. All the components of the cell were shaped as small cylinders assembled as a sandwich in which the electrolyte is in the middle. The electrolyte is a polished disk of CaF_2 monocrystal (Crismatec, France) (111) oriented, 2 mm thick, and 8 mm diameter.

The electrodes were prepared in a glove box filled with inert and dry atmosphere according to the criterion of establishing the polyphasic coexistence through a close contact among the powder particles. Following the well-established standard procedure, the pure solid phases, as fine powders, have been mixed in acetone and, after evaporation of the solvent, pressed in a stainless steel mould for obtaining cylinders 6 mm diameter × 3 to 5 mm height. Graphite, CrF_2, and Cr_3C_2 were pure powder chemicals (99%, 1−2 μm; 97%, 80 mesh; 99%, 325 mesh, respectively) from Aldrich. The weight ratio between graphite or MWCNTs, CrF_2, and Cr_3C_2 was about 1:1:1. The pressed mixtures were sintered at 800 °C for 24 h under a stream of electronic-grade argon. The surfaces of electrodes were gently polished in such a way as to be flat and in perfect contact with the electrolyte surfaces. The total length of the cells was never greater than 12 mm. Mo wires up to the feedthrough of the furnace flange realized the electrical leads. The temperature was measured by two S-type (Pt/Pt−Rh 10%) thermocouples which were calibrated against the melting of pure Au. Before starting the emf measurements, the system was carefully flushed with Ar (O_2 < 1 ppm, H_2O < 1 ppm) and then outgassed by following a standard procedure, which does not allow an increase in the temperature of the cell if the pressure inside the furnace is greater than 1×10^{-6} mbar. This procedure requires at least 2 days. The total pressure during the experiment is maintained below 1×10^{-7} mbar. A high impedance preamplifier (10^{15} ohm, typical bias current 40 fA) connected to one of the analog input channels of a data logger was used for the emf measurements. The total accuracy in reading the emf was less than 50 μV. The furnace temperature, pressure, and emf were read by the data logger connected to a personal computer. The stability of the temperature of the furnace at the set temperature was always within 1 K. The temperature changes throughout the experiments were performed by programmed ramps with a slope of |2| K/min.

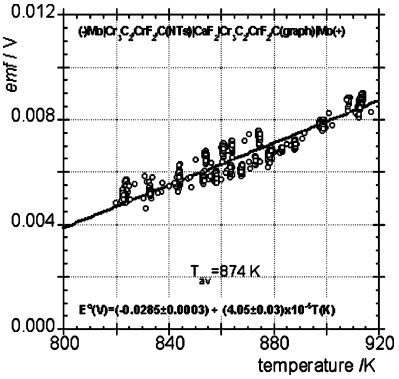

Figure 4. Cumulative emf versus T values for cell: Mo/Cr_3C_2,CrF_2, C″/CaF_2s.c./Cr_3C_2,CrF_2, C′/Mo. C′ ≡ graphite and C″ ≡ MWCNTs.

2.3. DSC Measurements. The DSC-TG measurements were carried out by a Netzsch STA PC 409 Luxx (Germany) thermal analyzer (DSC sensitivity = 0.16 μV mW^{-1}; TG resolution = 2 μg; temperature measurement range from room temperature to 1500 °C; temperature sensor: S-type thermocouple) and using two 0.085 cm^3 alumina crucibles both for reference and sample under flowing Ar of electronic grade. Throughout the measurements, the heating rate was always set at 5 °C min^{-1}.

To determine the enthalpy of transformation B, the reaction of formation of manganese carbide Mn_7C_3 was chosen because the DSC measurements were reproducible both with graphite and MWCNTs. The stoichiometric mixture of Mn powder (99%, ≈ 80 mesh, from Aldrich) with graphite or MWCNTs was prepared by mixing both powders in agate mortar with some acetone additions. A few weighed milligrams of the powder mixture were gently pressed on the bottom of the crucible to improve the heat exchange. Both crucibles were topped with their own alumina cups having a small hole for outgassing.

3. Results

The standard emf values, E^o, of cell A in which C′ ≡ graphite and C″ ≡ MWCNTs are reported in Figure 4 as function of the absolute temperature. Each point represents the average value of the acquired data at constant temperature. The standard deviation is within the point size (≤|0.1|mV). Several runs were performed each of them constituted by stepwise isotherms, each one lasting at least 5 h and scanning up and down the temperature range. The temperature step was within ± 20 K, and the heating rate was ± 2 K min^{-1}. The best fitting line equation in the 820−920 K range is

$$E^o\,(\mathrm{V}) = (-0.0285 \pm 0.0003) + (4.05 \pm 0.03) \times 10^{-5} T\,(\mathrm{K}) \quad (1)$$

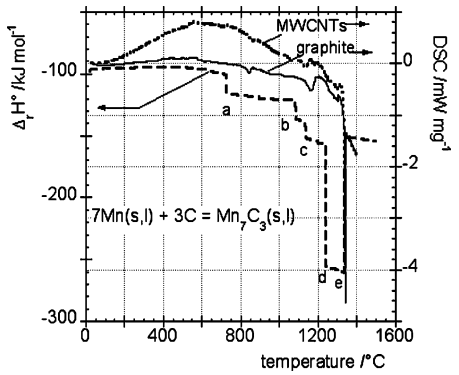

Figure 5. (Right scale) Differential scanning calorimetry (DSC) for the Mn_7C_3 formation starting from stoichiometric mixtures of Mn/graphite and Mn/MWCNTs. (Left scale) The tabulated[18] data of formation enthalpy of Mn_7C_3 are reported.

with $R = 0.94951$. Therefore, the thermodynamic quantities associated to transformation B, that is, graphite = MWCNTs, are

$$\Delta_r S^o = 3F(\partial E^o/\partial T)_P = 3F(4.05 \pm 0.03) \times 10^{-5} = 11.72 \pm 0.09\ \mathrm{JK^{-1}\,mol^{-1}} \quad (2)$$

$$\Delta_r H^o = 3F[E^o - T(\partial E^o/\partial T)_P] = -3F(-0.0285 \pm 0.0003) = 8.25 \pm 0.09\ \mathrm{kJ\ mol^{-1}} \quad (3)$$

$$\Delta_r G^o = -3FE^o = (8250 \pm 90) - (11.72 \pm 0.09)T\ \mathrm{J\ mol^{-1}} \quad (4)$$

where F is the Faraday constant.

The DSC measurements were performed by comparing the formation enthalpy change, $\Delta_f H^o$, of $Mn_7C_3(s)$ obtained starting from graphite or MWCNTs. Transformation B is again obtained when both formation reactions of $Mn_7C_3(s)$ are considered:

$$\frac{7}{3}\,\mathrm{Mn(s,l)} + \mathrm{C(graphite)} = \frac{1}{3}\mathrm{Mn_7C_3(s)} \qquad \frac{1}{3}\Delta_f H^o(\mathrm{G})$$

$$\frac{1}{3}\,\mathrm{Mn_7C_3(s)} = \frac{7}{3}\,\mathrm{Mn(s,l)} + \mathrm{C(MWCNTs)} \qquad -\frac{1}{3}\Delta_f H^o(\mathrm{M})$$

$$\mathrm{C(graphite)} = \mathrm{C(MWCNTs)} \qquad \Delta_r H^o = \frac{1}{3}\,[\Delta_f H^o(\mathrm{G}) - \Delta_f H^o(\mathrm{M})] \quad (5)$$

The formation of $Mn_7C_3(s)$ was selected because the melting of Mn, the carbide formation, and its melting occur in the same operative temperature range of the thermal analyzer. This ensures that (i) the formation of carbide is facilitated because graphite or MWCNTs react with a melted phase, that is, Mn-(l); (ii) a better heat transfer occurs caused by the melted phase; (iii) reliability checks can be performed during the experiment by comparing the transition temperatures and enthalpies with data reported in literature.[18] Figure 5 shows the typical DSC curves (right scale) from room temperature to 1500 °C obtained during the formation of $Mn_7C_3(s)$, starting from stoichiometric mixtures of Mn with graphite or MWCNTs. In the same figure,

(18) Belov, G. V.; Iorish, V. S.; Yungman, V. S. *IVTANTHERMO for Windows; database of thermodynamic properties of individual substances and thermodynamic modeling software*, version 3.0; Glushko Thermocenter of Russian Academy of Sciences: Moscow, Russia, 2005.

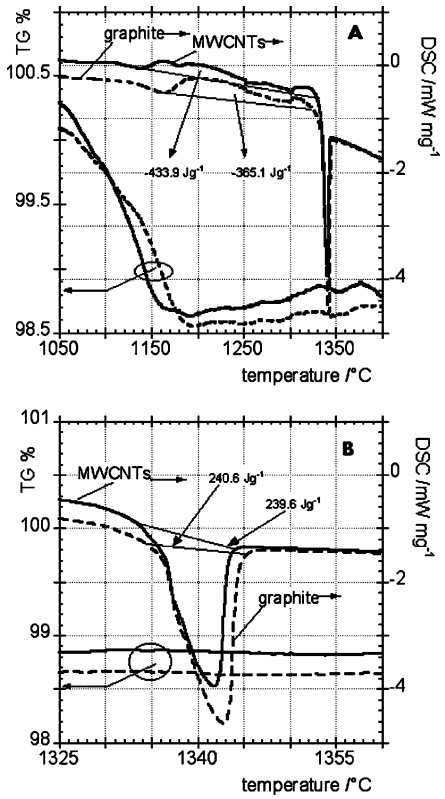

Figure 6. (A) (Left scale) Magnification of the thermogravimetry (TG) in the temperature window of Mn_7C_3 formation starting from stoichiometric mixtures of Mn/graphite and Mn/MWCNTs. (Right scale) Magnification of DSC in the temperature window of Mn_7C_3 formation starting from stoichiometric mixtures of Mn/graphite and Mn/MWCNTs. (B) (Left scale) Magnification of thermogravimetry (TG) in the temperature window of the Mn_7C_3 melting. (Right scale) Magnification of DSC in the temperature window of the Mn_7C_3 melting.

Table 1. Features of the Transitions Shown in Figure 5[a]

	transition	T_{tr}/°C	$\Delta_{tr}H^o_T$/kJ mol^{-1}
a	Mn(α) → Mn(β) b.c.c. → b.c.c.	726.5	2.2
b	Mn(β) → Mn(γ) b.c.c. → f.c.c.	1086.3	2.2
c	Mn(γ) → Mn(δ) f.c.c. → b.c.c.	1136.3	1.9
d	Mn(δ) → Mn(l)	1243.6	14.1
e	$Mn_7C_3(s) \rightarrow Mn_7C_3(l)$	1339.7	110.0

[a] The values of $\Delta_{tr}H^o_T$ from **a** to **d** should be multiplied by 7 to obtain the values reported in the same figure (left scale).

on the left scale, is plotted the formation enthalpy, $\Delta_f H^o$, of Mn_7C_3 as function of temperature, as given in a thermodynamic database.[18] The transitions shown in Figure 5, named from *a* to *e*, are reported in Table 1. The set of DSC data is given in Table 2 , and two magnifications of a typical DSC/TG experiment are reported in Figure 6A and 6B, respectively. The former displays the exothermic DSC changes (right scale) due to $Mn_7C_3(s)$ formation, the latter displays the endothermic changes due to the $Mn_7C_3(s)$ melting. Starting from around 1000 °C, a negligible weight loss (left scale) was found caused by the vaporization of Mn. In fact, at 1000 °C, the Mn vapor pressure is quite high being 2.6 Pa.[18] Just $Mn_7C_3(s)$ was formed; the weight loss stopped because liquid Mn disappeared, and the vapor pressure of $Mn_7C_3(s,l)$ is very low. According to data reported in Table 2, $\Delta_r H^o_{1500}(\mathrm{DSC}) = (1/3)MW[{}_fQ^o_{1500}(\mathrm{G}) - {}_fQ^o_{1500}(\mathrm{M})] = 9.7 \pm 0.8$ kJ mol^{-1}.

Table 2. DSC Data for Reaction $7Mn(s,l) + 3C = Mn_7C_3(s)$ and Transformation $Mn_7C_3(s) = Mn_7C_3(l)$ in Columns 2, 3, and 4, Respectively

C	$-{}_rQ^o_{1500}$(G) J g^{-1} (exo)	$-{}_rQ^o_{1500}$(M) J g^{-1} (exo)	${}_mQ^o_{1613}$ J g^{-1} (endo)
graphite	365.1	-	240.6
graphite	358.0		252.6
graphite	362.3		239.6
MWCNTs		423.2	225.6
MWCNTs		436.2	215.2
MWCNTs		433.9	200.3
average	362 ± 2	431 ± 4	229 ± 8

MW is the formula weight of Mn_7C_3 (420.566 g mol^{-1}). The values in square brackets are given in Table 2.

4. Discussion

We obtained data of graphite = MWCNTs transformation by two independent techniques but at different temperatures. Data obtained through the emf measurements are referred to the average temperature of 874 K whereas DSC data should be referred to 1500 K this temperature being approximately in the middle of the exothermic area evaluated (see Figure 6A). To compare the values, the knowledge of the heat capacity, C_p, versus T of graphite and MWCNTs should be available. Unfortunately, neither theoretical nor experimental C_p versus T data exist for MWCNTs in a wide temperature range up to the high temperatures. In general, a few papers deal with such field: some of them are theoretical ones,[19−22] and SWCNTs are mostly treated. Four papers[23−26] can be found on experimental C_p measurements, all ones below room temperature, and three of them[23,25,26] concern MWCNTs in the temperature ranges 0.6−210 K, 1.8−250 K and 10−300 K, respectively.

Through a careful inspection of the above literature, some information can be drawn which is useful for the calculation of the thermodynamic quantities as function of temperature. It can be summarized as follows:

(i) Above 60 K graphite and MWCNTs have practically the same C_p versus T trend which is linear up to 300 K.[27]

(ii) Below 60 K, the specific heats deviate because of the different low temperature acoustic phonon densities of states, and the C_p value of MWCNTs is always higher than graphite. At 2 K, $C_{p_{MWCNTs}}/C_{p_{graphite}} \approx 6$. In graphite the dimensional crossover from 2D to 3D behavior occurs in the temperature range 50−80 K.[28]

(iii) For MWCNTs below 40 K the long wavelength acoustic phonon modes perpendicular to the tube axis begin to dominate, in addition to the acoustic longitudinal and twist phonon modes, and the interlayer coupling in the nanotubes becomes significant. The change in the slope of the curve at about 35 K confirms the dimensional crossover.

(19) Xiao, C.; On Chan, H. S.; Xu, G. Q.; Lim, K. T.; Lin, J. *Appl. Phys. Lett.* **2004**, *84*, 1677.
(20) Hepplestone, S. P.; Ciavarella, A. M.; Janke, C.; Srivastava, G. P. *Surface Sci.* **2006**, *600*, 3633.
(21) Li, C.; Chou, T. W. *Materials Science and Engineering A* **2005**, *409*, 140.
(22) Popov, V. N. *Phys. Rev. B* **2002**, *66*, 153408.
(23) Mizel, A.; Benedict, L. X.; Cohen, M. L.; Louie, S. G.; Zettl, A.; Budraa, N. K.; Beyermann, W. P. *Phys. Rev. B* **1999**, *60*, 3264.
(24) Hone, J.; Batlogg, B.; Benes, Z.; Johnson, A. T.; Fisher, J. E. *Science* **2000**, *289*, 1730.
(25) Masarapu, C; Henry, L. L.; Wei, B. *Nanotechnology* **2005**, *16*, 1490.
(26) Yi, W.; Lu, L.; Dian-lin, Z.; Pan, Z. W.; Xie, S. S. *Phys. Rev. B* **1999**, *59*, R9015.
(27) De Sorbo, W.; Tyler, W. W. *J. Chem. Phys.* **1953**, *21*, 1660.
(28) Alexander, M. G.; Goshorn, D. P. *Phys. Rev. B* **1980**, *22*, 4535.

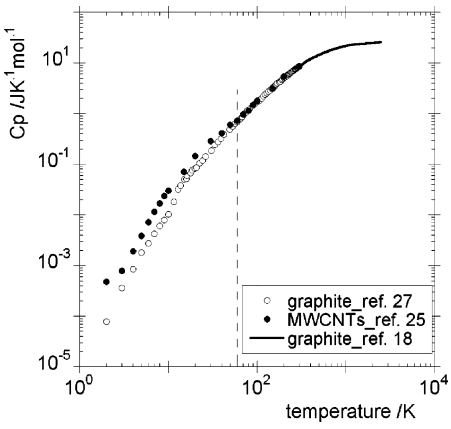

Figure 7. Heat capacity, C_p, of MWCNTs[25] and graphite[27,28] from 2 to 2500 K. From $T \geq 60$K, the C_p temperature dependency of MWCNTs and graphite becomes practically the same.

(iv) Below 35 K, the C_p curve of MWCNTs is approximately given by αT^n with n and α changing, respectively, from 2.2 to 3 and from 0.017 to 0.003 as T decreases. Only below 5 K, MWCNTs behave as an ideal Debye solid the electronic specific heat being negligible with respect to the phonon specific heat.

(v) Theoretical calculations[21] on MWCNTs show that C_p versus T curve is scarcely influenced by the chirality, outer diameter, and the number of walls, whereas it depends strongly of the length, especially at high temperatures. At fixed T, C_p increases with length.

The log−log plot of Figure 7 shows the whole C_p trend of MWCNTs and graphite in the range from 2 to 2500 K. Therefore, $\Delta_r H^o_{298}$ of transformation B is given by

$$\int_{\bar{T}}^{298} \mathrm{d}\Delta_r H^o(T) = \int_{\bar{T}}^{298} (C_{p_{MWCNTs}} - C_{p_{graphite}})\,\mathrm{d}T = -(H^o_T - H^o_{298})_{MWCNTs} + (H^o_T - H^o_{298})_{graphite} \approx 0 \quad (6)$$

where $(H^o_T - H^o_{298})$ is the enthalpy function and $\bar{T}$ the average experimental temperature. So we can write that $\Delta_r H^o_{298}(\mathrm{emf}) \approx \Delta_r H^o_{874}(\mathrm{emf})$ and $\Delta_r H^o_{298}(\mathrm{DSC}) \approx \Delta_r H^o_{1500}(\mathrm{DSC})$. The average value of $\Delta_r H^o_{298}$ from both the techniques is 9.0 ± 0.8 kJ mol^{-1}.

To calculate $\Delta_r S^o_{298}$ it is necessary to consider that

$$\Delta_r S^o_{\bar{T}} = \Delta_r S^o_0 + [\int_0^{298} C_{p_{MWCNTs}}\,\mathrm{d}\ln T - \int_0^{298} C_{p_{graphite}}\,\mathrm{d}\ln T] + (S_{\bar{T}}{}^o - S_{298}{}^o)_{MWCNTs} - (S_{\bar{T}}{}^o - S_{298}{}^o)_{graphite} \quad (7)$$

Due to the same trend of C_p versus T for graphite and MWCNTs above 60 K (see Figure 7), eq 7 becomes

$$\Delta_r S^o_{\bar{T}} \approx \Delta_r S^o_0 + [\int_0^{60} C_{p_{MWCNTs}}\,\mathrm{d}\ln T - \int_0^{60} C_{p_{graphite}}\,\mathrm{d}\ln T] \quad (8)$$

The value of the integrals in eq 8 was found by the experimental C_p/T versus T data of MWCNTs[25] and graphite,[27,28] respectively. The respective values are 0.45 and 0.36 JK^{-1} mol^{-1}. Therefore, $\Delta_r S^o_{\bar{T}} \approx \Delta_r S^o_{874} \approx \Delta_r S^o_{298} = \Delta_r S^o_0 + 0.09$, where $\Delta_r S^o_{298} = 11.72 \pm 0.09$ JK^{-1} mol^{-1} is given by eq 2. It follows that $\Delta_r S^o_0 = 11.63 \pm 0.09$ JK^{-1} mol^{-1} and, consequently, being for graphite $S^o_0 = 0$, S^o_0 (MWCNTs) = $\Delta_r S^o_0$. This residual entropy of MWCNTs is the sum of at least three terms:

$$S^o_0(\mathrm{MWCNTs}) = S^o_0(\mathrm{c}) + S^o_0(\mathrm{m}) + S^o_0(\mathrm{d}) \quad (9)$$

Table 3. Calculated $\Delta_r H_0^o$ Values for Transformation Graphite→MWCNTs as Reported in Literature[10] for Two Extreme Layer Interaction Energies, W_L[a]

		W_L		
R_i /nm	n_L	−4.10	kJ mol^{-1}	−21.0
		$\Delta_r H_0^o$		
0.339	2	4.40		13.60
	8	6.47		8.26
	32	6.49		6.27
1.695	2	8.60		17.75
	8	6.93		8.69
	32	6.53		6.31
	≫32		*9.0 ± 0.8*	

[a] Distance between layers is 0.339 nm and nanotubes are 10 nm long. Values in italics, this work.

where c, m, and d stand, respectively, for configuration, mixing, and defectivity. S_0^o(c) is due to the number of microstates created by the positioning of each carbon atom in a bended graphene layer with respect to the C atoms of the adjacent layer. Besides, the closing of each graphene layer to generate a tube, implies the matching of its edges. This becomes possible only if some hexagons, p_6, are replaced by pentagons, p_5, and heptagons, p_7. According to the Euler theorem in topology,[29] the presence of p_5 implies an equal number of p_7. Zhang et al.[11] treated such as system of p_5 and p_7 in the p_6 network as an ideal solution, that is, as a complete random distribution, and they calculated accordingly the entropy of mixing.

Therefore, $S_0^o(\mathrm{m}) = -k_B P[x \ln x + (1-x)\ln(1-x)]$, where $x = (p_5 + p_7)/P$, P being the total number of carbon polygons. For ropes of SWCNTs, it was calculated[11] that the minimum of the free energy at 1500 K is found when $x = 6.845 \times 10^{-4}$ in tubes with radii equal to 0.6958 nm. Further contribution to the residual entropy is given by S_0^o(d) owing to the various types of defects existing in real MWCNTs.

The $\Delta_r H_{298}^o$ values obtained through the two independent techniques are in good agreement and, to discuss them with reference to literature, their average value equal to 9.0 ± 0.8 kJ mol^{-1} will be considered. Because of the higher complexity of MWCNTs with respect to SWCNTs, the theoretical calculations are practically absent in literature and the task of determining the thermodynamics of the graphite/MWCNTs transformation has not yet been considered. Setton[10] treated the problem of computing the enthalpy of transformation from graphite to MWCNTs by using the Lennard-Jones (6,12) empirical energy function. He calculated both the intralayer (or carbon−carbon) and layer−layer interactions as a function of the number of layers, n_L, distance, d_L, between them, and innermost radius, R_i, of nanotube. Apart from the intrinsic approximations in the empirical energy function, the large uncertainty in the W_L value of graphite implies also some uncertainty in the graphite W_B energy because the relationship

$$-\Delta_v H_0^o = W_L + W_B \qquad (10)$$

has to be satisfied. $\Delta_v H_0^o = 710.51$ is the standard vaporization enthalpy of graphite at 0 K used in reference 10 (a more recent and accurate value[18] is −711.19 kJ mol^{-1}). According to Setton,[10] for MWCNTs having $d_L = 0.339$ and 10 nm long, $\Delta_r H_0^o$, at fixed n_L and R_i, changes significantly depending on the adopted value of W_L as shown in Table 3. What emerges clearly by inspecting Table 3 is that when n_L becomes sufficiently large, $\Delta_r H_0^o$ tends to a common value whatever is R_i and W_L. The average among the four values at $n_L = 32$ gives $\Delta_r H_0^o = 6.40$ kJ mol^{-1}. Looking at Figure 1b,c, the MWCNTs used in this work have $n_L \gg 32$ and $R_i \approx 1.7$ nm but their length is 3 order of magnitude higher than the length value used in the above literature calculations. To compare correctly the calculated enthalpy of transformation, $\Delta_r H_0^o$, with the experimental $\Delta_r H_{298}^o$, it is necessary to correct it at 0 K through the equation

$$\Delta_r H_0^o = \Delta_r H_{298}^o - (H_{298}^o - H_0^o)_{\mathrm{MWCNTs}} + (H_{298}^o - H_0^o)_{\mathrm{graphite}} \qquad (11)$$

As stated before, at $T \geq 60$ K, $C_{p\mathrm{MWCNTs}} \cong C_{p\mathrm{graphite}}$, then eq 11 can be written as

$$\Delta_r H_0^o \approx \Delta_r H_{298}^o - (H_{60}^o - H_0^o)_{\mathrm{MWCNTs}} + (H_{60}^o - H_0^o)_{\mathrm{graphite}} \qquad (12)$$

Since the $(H_{60}^o - H_0^o)_{\mathrm{MWCNTs}}$ and $(H_{60}^o - H_0^o)_{\mathrm{graphite}}$ values are, respectively, 0.018 and 0.014 kJ mol^{-1}, eq 12 becomes $\Delta_r H_0^o \approx \Delta_r H_{298}^o = 9.0 \pm 0.8$ kJ mol^{-1} the difference being between the enthalpy functions within the limits of the whole uncertainty on $\Delta_r H_{298}^o$. Looking at Table 3, one observes that the $\Delta_r H_0^o$ value determined is slightly higher than the lowest calculated value. It needs to be noted that the theoretical calculations were performed for 10 nm long MWCNTs, and their turbostraticity was not considered. The MWCNTs tested are a thousand times longer; turbostraticity exists though we are not able to quantify it. These aspects are probably responsible for the above difference in $\Delta_r H_0^o$ values.

From the above thermodynamic quantities, calculated at 298 K, $\Delta_r G_{298} = \Delta_r G_{298}^o = 5.5 \pm 0.8$ kJ mol^{-1}. Therefore, the transformation from graphite to MWCNTs is unfavorable, as expected. According to the reversible experimental data (emf), the transformation becomes spontaneous at $T > 704 \pm 13$ K.

On thermodynamic basis, it is now possible to calculate the standard free energy change of decomposition, $\Delta_d G^o$, of a light hydrocarbon, say CH_4, when the MWCNTs are formed. Combining equations

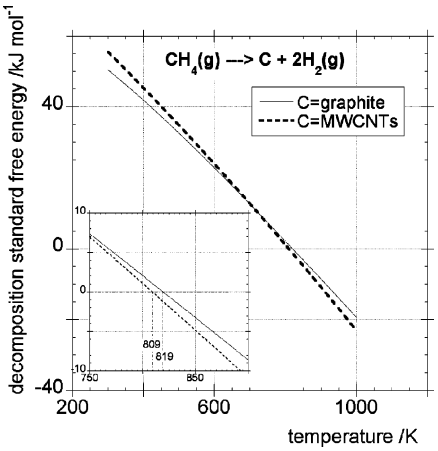

Figure 8. Standard free energy changes as function of the absolute temperature for methane decomposition in the cases of graphite or MWCNTs formation. The magnification in the inset shows the temperatures at which the decompositions become favored by thermodynamics.

(29) Do Carmo, M. P. *Differential Geometry of Curves and Surfaces;* Prentice Hall: Englewood Cliffs, NJ, 1976.

$$\begin{array}{lll} CH_4(g) = C(MWCNTs) + 2H_2(g) & & \Delta_d G_1^o \\ C(graphite) + 2H_2(g) = CH_4(g) & & \Delta_f G_2^o \\ \hline C(graphite) = C(MWCNTs) & & \Delta_r G_3^o \end{array} \qquad (13)$$

it follows that $\Delta_d G_1^o = \Delta_r G_3^o - \Delta_f G_2^o$, where $\Delta_r G_3^o$ is given by eq 4 and $\Delta_f G_2^o$ is tabulated.[18] Figure 8 shows the result of this calculation. The decomposition of methane to form MWCNTs is thermodynamically favored at temperatures above 809 K, 10 K below when the decomposition involves graphite. This temperature is within the optimum temperature range in which our MWCNTs grow on the catalyst[12] according to the proposed mechanism.[13]

5. Conclusion

In summary, we showed the thermodynamics of the transformation from graphite to MWCNTs through two independent experimental techniques. We derived both the enthalpy and entropy of this transformation establishing the lower temperature at which it becomes spontaneous. We obtained also the residual entropy of MWCNTs that coincides practically with the standard entropy change of the transformation. As far as the authors' knowledge, the above data are not yet reported in literature. The reliability of the experimental data is supported by the value of the transformation enthalpy, which was found practically the same, within the experimental errors, by making use of emf and DSC measurements.

Acknowledgment. The authors are very grateful to Prof. G. Capannelli and Mr. C. Uliana of the Department of Chemistry and Industrial Chemistry of the University of Genoa, Italy, for the TEM analyses they performed.

JA072120D